Supporting Information for

Revisiting the Promise of Bi-layer Graded Cathodes for Improved Li-ion Battery Performance

Authors:

Ridwanur Chowdhury[a*], Yan Zhao[b], Yuhua Xia[a] , Mengzheng Ouyang[a*], Nigel Brandon[a], Aayan Banerjee[c]

[a]Department of Earth Science and Engineering, Imperial College London, UK
[b]Department of Mechanical Engineering, Imperial College London, UK
[c]Catalytic Processes and Materials, Faculty of Science and Technology, University of Twente, Netherlands

XCT Scanning Settings

Table S1. XCT imaging settings

Voltage	Power	Detector	Pixel Size	No. of Projection	Field of View	Exposure time
80 kV	7W	40X	353 nm	3201	318 x 343 x 332 µm	6 seconds

Coin Cell Configuration and XRD Patterns of NMC532 Powder Samples

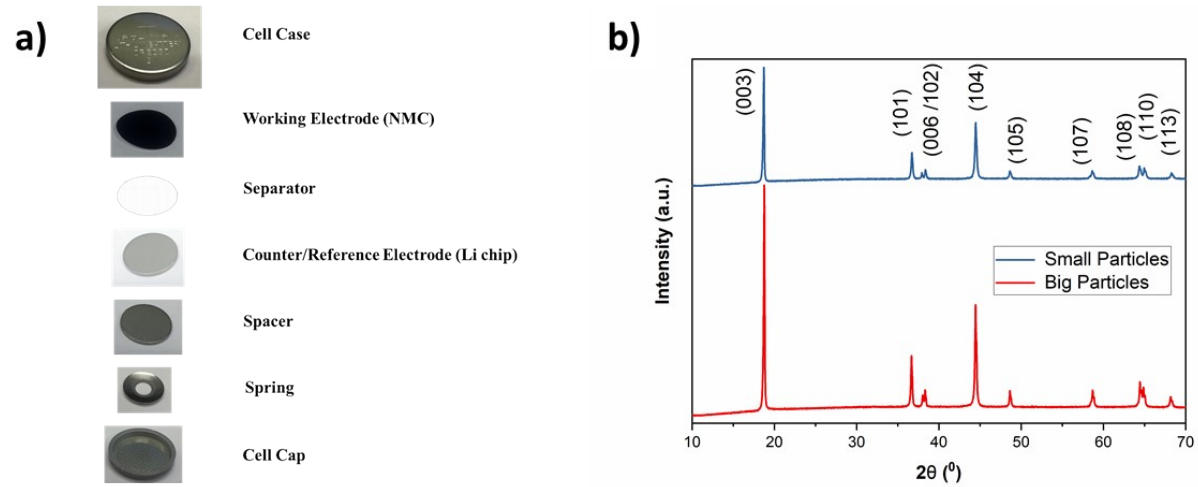

Fig. S1. (a) Half-cell assembly for cycling and EIS measurement and (b) XRD patterns comparison for as-received (big particles) and ball-milled (small particles) samples.

2D Image Analysis of Top Layer Consisting of Big Particles

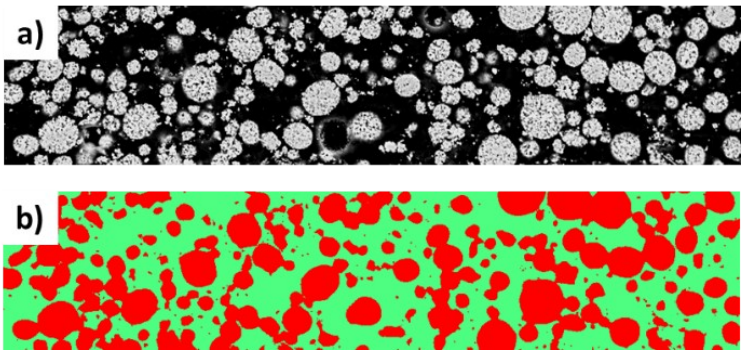

Fig. S2. (a) Cross-sectional SEM image and (b) segmented image of the top layer composed of big particles.

The area of the top layer (Fig. S2 (a)) consisting of big particles is cropped from Fig. 3(e) for porosity estimation purpose. The two-phase segmented micrograph in Fig. S2 (b), red represents solid-phase and green represents pore phase.

Structural Characterization of the Monolayer Electrodes

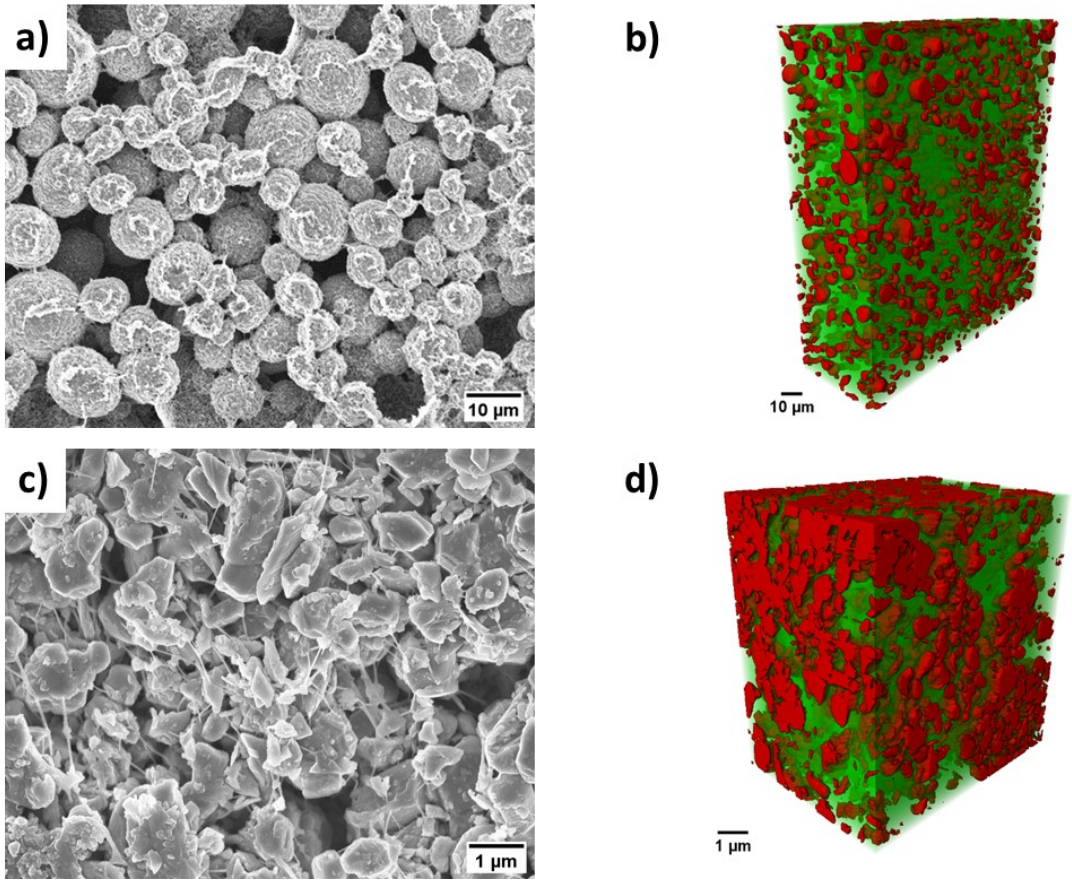

Fig. S3. SEM images and 3D rendering of the reconstructed single layer electrodes with (a-b) big and (c-d) small particles.

The top-view SEM images of the single layer electrodes show no binder migration, CB deposition and CB agglomeration at the electrode surface due to drying conditions. The 3D volume of the SLC1 and SLC2 were reconstructed by using the Avizo software, where green is the pore phase and red is the AM phase.

Equivalent Electronic Circuit (EEC) Model

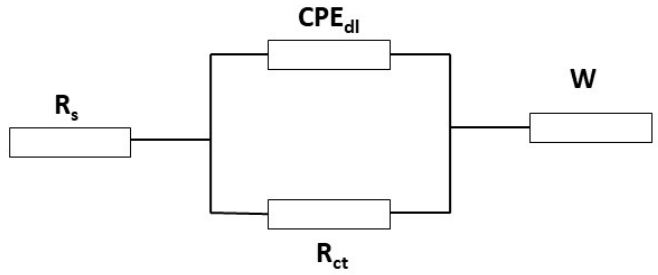

Fig. S4. EEC circuit model used for EIS experimental data fitting.

The used EEC does not consider the contribution from CEI since the first semi-circle (related to film resistance) over the high frequency range (100kHz-10Hz) was not observed after three formation cycles. Therefore, a simplified EEC model is adopted based on previous studies on NMC, as referred in the manuscript.

Effect of Slurry Drying Temperature

Fig. S5 (a) and (c) show the top-view SEM images of the electrodes with big particles dried at 60°C. These SEM images confirm the surface of the secondary AM particles are covered by CB and binder. Similar surface morphology is observed for the electrodes with small particles as shown in Fig. S5 (e). Crack formation and binder migration is observed for both big (Fig. S5 (b, d)) and small particles (Fig. S5 (f)) when the temperature is increased to 90°C.

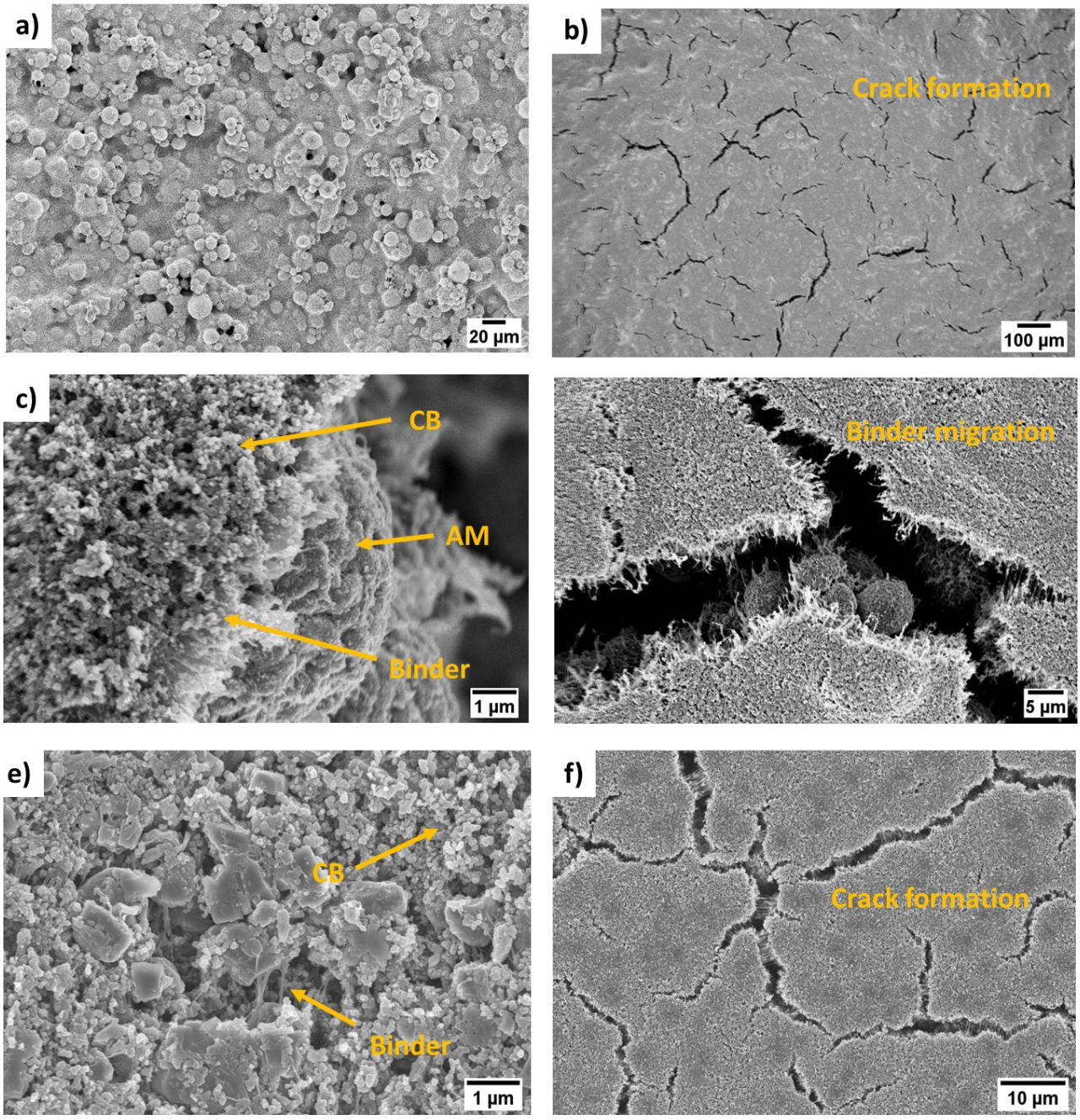

Fig. S5. SEM images of electrodes dried at (a, c, e) 60°C and (b, d, f) 90°C. Electrodes with big particles in (a, b) low and (c, d) high magnification. (e-f) Electrodes with small particles